I&EC research
Industrial & Engineering Chemistry Research

pubs.acs.org/IECR

Article

Analysis of Polycyclic Aromatic Hydrocarbon Emissions from a Pilot Scale Silicon Process with Flue Gas Recirculation

Kamilla Arnesen,* Kurian J. Vachaparambil, Vegar Andersen, Balram Panjwani, Katarina Jakovljevic, Ellen Katrin Enge, Heiko Gaertner, Thor Anders Aarhaug, Kristian Etienne Einarsrud, and Gabriella Tranell*

Cite This: https://doi.org/10.1021/acs.iecr.2c04578

ABSTRACT: Flue gas recirculation (FGR) is a method used in several industries to control emissions and process conditions, such as NO_x reduction and temperature levels, and increase the CO_2 concentration in the off-gas, to be better suited for methods of carbon capture. In this study, the influence of FGR, varying levels of flue gas flow and oxygen concentration on the emissions of polycyclic aromatic hydrocarbons (PAHs) was investigated during Si alloy production. In addition, computational fluid dynamics (CFD) modeling was performed using OpenFOAM for combustion of C_2H_2 and H_2 with varying O_2 levels to simulate FGR and to gain better insight into the impact of furnace operations on the PAH evolution. Experimental results show that increasing FGR (0−82.5%) and decreasing levels of oxygen (20.7−13.3 vol %) increase the PAH-42 concentration from 14.1 to 559.7 $\mu g/Nm^3$. This is supported by the simulations, where increased formation of all PAHs species was observed at high levels of FGR, especially for the lighter aromatic species (like benzene and naphthalene), due to the lower availability of oxygen and the reduction in temperature. Residence time was identified as another key parameter to promote complete combustion of PAHs. Benzene oxidation can be prevented with temperatures lower than 1000 K and residence times smaller than 1 s, while complete oxidation is found at temperatures of around 1500 K.

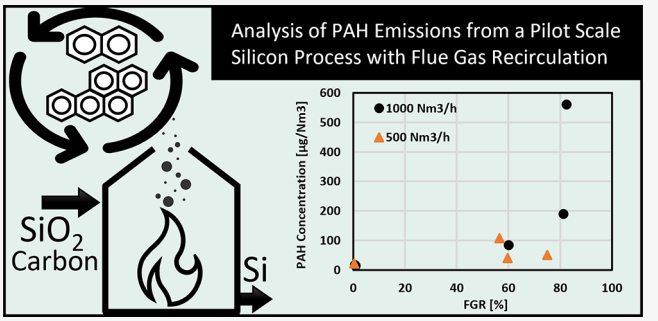

INTRODUCTION

Polycyclic aromatic hydrocarbons (PAHs) are a group of organic molecules consisting of two or more fused aromatic rings. They occur naturally in petroleum and resin products and can be produced by incomplete combustion of organic matter. Natural sources of PAHs are forest fires and volcanic activity, and anthropogenic sources can be burning of biomass and oil, production of coke and the use of carbon in industrial processes. PAHs are classified as persistent organic pollutants, and some species are known to be mutagenic and carcinogenic.[1] The European Union has agreed on a General Union Environment Action Program to reduce exposure and emissions of PAHs in 2013.[2] In 2004 the global emission of PAHs were estimated to be 520 Gg/y, using reported emissions and emission factors, where combustion of biofuel and wildfire account for 56.7% and industrial activity such as coke production is less than 10%.[3] The focus is often on the EPA-16 PAH, which is a list with components consisting solely of aromatic rings. The list was established in the 1970s and has become the standard for measuring and reporting PAH emissions. An upside to this is that keeping track of changes and trends over time has becomes more convenient. Some argue that the EPA-16 list is not optimal when measuring the exposure of toxic emissions, as some compounds have a short life span and decompose quickly when exposed to sunlight while other more stable compounds are not included, such as alkylated or substituted PAH.[4]

Mixtures of PAHs are often characterized based on ratios to identify suspected emission sources, either by isomer pairings or larger fractions within the mixture.[5] The process and conditions are crucial for which PAHs are formed and destroyed, such as raw material and temperature. A high temperature process such as flame oxidation (e.g., methane combustion at 2000 °C) often produces high molecular weight (HMW) PAHs as the conditions can produce radicals that react and form stable PAHs. This is often called pyrogenic combustion. At lower temperatures (e.g., diesel engine runoff emission) PAHs of low molecular weight (LMW) are formed and can be referred to as petrogenic sources.[6] An example of

Received: December 21, 2022
Revised: April 20, 2023
Accepted: April 21, 2023

such a ratio used for separating between pyrogenic and petrogenic sources are the ratios between phenanthrene (Phen) and anthracene (Anth), where Phen is more thermodynamically stable and is therefore a more likely product from a high temperature combustion process. Fluoranthene (Fla) and pyrene (Py) is another such example, and the two ratios are often studied as a pair to better identify source emissions.[7,8] A ratio between LMW and HMW PAHs can also refer to the carbon source. LMW/HMW < 1 indicates a pyrogenic source with incomplete combustion of fossil fuel or wood, and a ratio >1 could indicate a petrogenic source including oil spill and petroleum products.[9]

A semiclosed submerged arc furnace (SAF) is commonly used to produce metallurgical grade silicon (MG-Si) through a carbothermal reduction, using a mix of coal, coke, charcoal and woodchips as the reductants. The carbon materials reduce the quartz to silicon alloy, by the overall reaction shown in eq 1, where σ is the Si yield, which gives the distribution between tapped Si and SiO leaving the furnace to react to SiO_2 (silica fume).[10]

$$SiO_2 + (1+\sigma)C = \sigma Si + (1-\sigma)SiO_{(g)} + (1+\sigma)CO_{(g)} \quad (1)$$

Silicon oxide (SiO) and carbon monoxide (CO) that reach the top of the furnace react with air to form silica fume and carbon dioxide (CO_2), respectively, in the furnace hood.[10] This affects the temperature at the charge surface in the furnace, which can reach 700 to 1300 °C. Because the SAF is semiclosed, the under pressure in the furnace drives the surrounding air into the furnace hood, diluting the furnace off-gas, which consist mainly of air with small amounts of CO_2 and other greenhouse gases, as well as PAHs. Off-gas temperatures can be 400 to 700 °C above the crust of the charge materials in contact with air, and the silica fume is typically captured using a bag-house filter at moderate temperatures of approximately 60 to 220 °C, depending on the filter type. PAHs are emitted from the furnace, either from the top of the gas permeable furnace charge material or through gas released during the tapping process. Typically these PAHs originate from pyrolysis and combustion of the carbon raw materials, electrodes and carbon paste.[11] Efficient pyrolysis of coal should result in the breakdown of large organic molecules to smaller hydrocarbons, and in efficient combustion the only products would be CO_2, H_2O, CO, etc. However, such complete degradation of coal rarely occurs, and organic compounds, including PAHs, are released during the reduction process. Work is being done to develop PAH reduced or PAH-free binder products to reduce emissions.[12] Apart from the PAH evolution driven by fuel containing PAHs, combustion of aliphatic fuels (like methane or acetylene) can also generate PAHs. To the best knowledge of the authors, the fuel bounded PAHs as well as the aliphatic fuels evolving from the carbon material in the furnaces are not well understood. A study by Gaertner et al.[13] reported EPA-16 PAH emissions from the flue gas stack at a silicon plant in Norway to be 2 $\mu g/Nm^3$ in the off-gas and 1.81 ng/g EPA16-PAH on the dust (PM). Increased levels of PAH emissions were observed after a furnace restart. Reported emission levels vary between plants, and in 2020 Norwegian silicon and ferro-silicon producers reported between 0.35 kg/year and 296.39 kg/year EPA-16 PAH emissions to air and water from different plants to the Norwegian Environmental Agency.[14]

Flue gas recirculation (FGR) is a method to redirect parts of the process off-gas back to the furnace. It can be done to utilize components in the off-gas, increase energy efficiency by reducing heat losses, aid in process control, and as a way to concentrate off-gas species, such as CO_2, for further processing. The silicon industry is a candidate for carbon capture, and flue gas recirculation could increase the CO_2 concentration in the off-gas, adding to the capture efficiency.[15,16]

Exhaust gas recirculation (EGR) is an established method for reducing NO_x formation in engines by reducing the oxygen levels and the temperature and, with that, slowing down the combustion process.[17] Chen et al.[18] tested the effect of EGR to reduce emissions of persistent organic pollutants from diesel engines. This work show a 9 times increase in PAH by mass emission factors when the EGR was set to 5%. In the work of Abdelaal et al.,[19] FGR is used in an attempt to reduce NO formation from dimethyl ether fuel combusted by temperature decrease. In this case, NO is reduced, but for FGR above 20% a noticeable increase in CO and unburned hydrocarbons (UBHs) occurs from 0 to 0.45% and 0 to 650 ppm, respectively, at 40% FGR and 3% O_2. Liu et al.[20] observed increased combustion efficiency of C_2H_4 in a fuel-rich flame between 1680 and 1820 K with EGR when studying PAH formation. A way to reduce PAH emissions from industrial processes requires its capture and treatment or ensuring a complete combustion.

In order to develop processes to ensure complete combustion of PAHs, an understanding of mechanisms that describe the evolution of PAH is important. Very briefly, PAH evolution can be summarized into formation of the first aromatic ring (C_6H_6) during combustion of aliphatic species, the growth into larger PAH and eventually the soot formation, and oxidation of these species into smaller aromatic rings and carbon dioxide. The main formation mechanisms are based on different reactants, where acetylene additions (e.g., HACA), vinyl acetylene additions (HAVA), and radical reactions with C1−C6 are usually in focus.[21] These are complex mechanisms involving hundreds to thousands of reactions; for example, the C_2H_2 combustion mechanism that includes PAH until $C_{20}H_{12}$ contains 112 species and 939 reactions.[22] For readers interested in understanding the PAH chemistry driving its evolution, it is recommended to refer to other works in literature like the review by Reizer et al.[21] Using computational fluid dynamics (CFD) (with a reaction mechanism treating PAH evolution) to model industrial processes is an ideal way to investigate the impact of furnace operations on the PAH evolution. For example, Panjwani et al.,[23] using a postprocessing technique based on CFD modeling, reported that temperature should exceed 800 °C for optimal combustion of 1-methylnaphthalene in addition to having a longer residence time >2 s (when compared to other process gases).

The objective of this study was to investigate the emissions of an extended list of PAHs, including alkylated and heterocyclic PAHs, from pilot scale silicon production and evaluate the effect of flue gas recirculation on the combustion conditions and resulting levels of PAHs. To gain better insight into the complex PAH evolution from the SAF, CFD modeling was performed using OpenFOAM for C_2H_2 and H_2 combustion with varying O_2 levels to simulate FGR.

EXPERIMENTAL AND MODELING METHODOLOGY

Pilot Furnace. A pilot scale one-phase submerged arc furnace was used for silicon production with flue gas

https://doi.org/10.1021/acs.iecr.2c04578
Ind. Eng. Chem. Res. XXXX, XXX, XXX−XXX

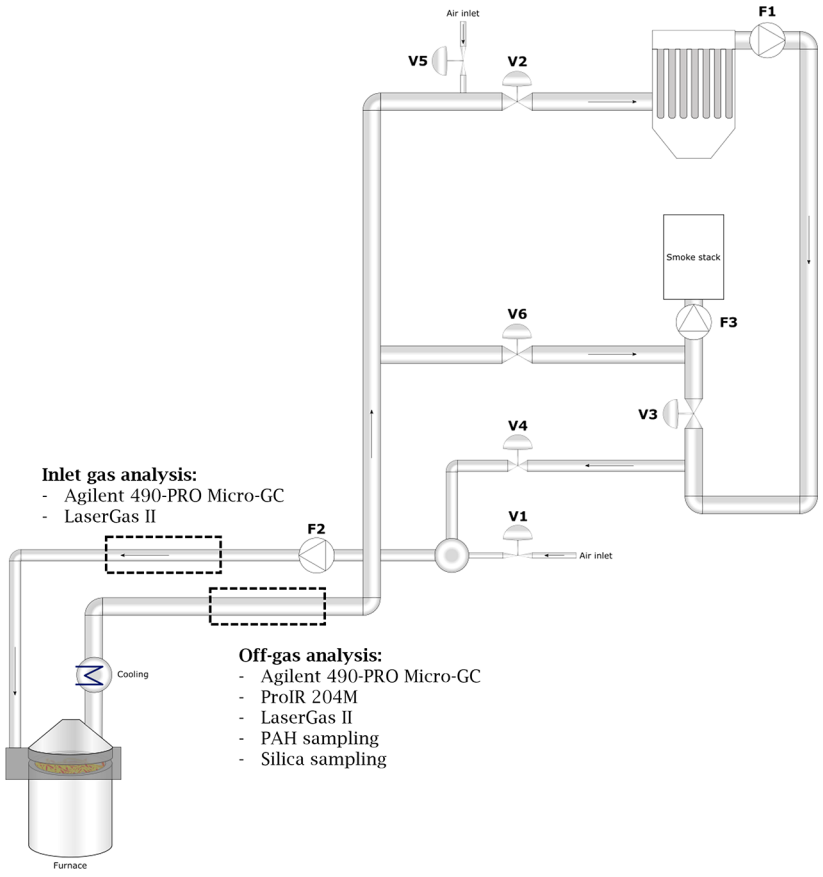

Figure 1. Silicon pilot SAF with a closed off-gas recirculating system. Placement of valves (V), fans (F) and location of various sampling systems are marked. Reprinted with permission from Andersen et al.[24] Copyright 2022 The Minerals, Metals & Materials Society.

recirculation over a 3-day period with continuous operations to investigate how FGR influenced PAH and off-gas composition from the silicon furnace. More details regarding the experiment can be found in the works of Andersen et al.[24,25] The furnace and off-gas system is illustrated in Figure 1. Power was supplied to the furnace thought a 6 in. graphite electrode (EG90, Tanso) at maximum 400 kVA. A mix of coal, coke, charcoal, woodchips and quartz made up the raw materials, which were supplied by an industrial partner. The materials were used as received, except for the woodchips, which were dried at 100 °C for 24 h. More information about the carbon raw materials is found in Table 1.

Table 1. Information about the Carbon Raw Materials Used in the FGR Pilot Experiments[a]

	Coal	Coke	Charcoal	Woodchips
Moisture (wt %)	10.8	11.7	4.7	4.8
Fix C (DB, wt %)	57.6	90.5	79.0	14.6
Ash (DB, wt %)	2.0	2.8	3.3	1.1
Volatiles (DB, wt %)	40.4	6.6	17.7	84.2
Share of C-mix (% Fix C)	40	15	30	15
Carbon (%DW)	78	90.8	83	50.7
Nitrogen (%DW)	1.58	1.68	0.39	0.2
Oxygen (%DW)	12	2.5	9.6	41.4
Hydrogen (%DW)	5.79	1.83	3.71	6.48
Sulfur (%DW)	0.05	0.42	0.05	0.11

[a]Analysis performed by ALS Scandinavia, Luleå, Sweden.

The furnace off-gas system was modified to achieve a closed off-gas system, which included a furnace hood, recycle, and redistribution system. After the off-gas exited the furnace and passed through a bag-house filter, a set of valves was used to determine if the off-gas should exit thought the smoke stack or be recirculated back to the furnace. The FGR ratio was set by the dilution factor between fresh air and recirculated off-gas.

The off-gas composition was analyzed during the experiment using different techniques, on both the furnace outlet and inlet. Gas composition (e.g., H_2, O_2, N_2, CO_2 and CH_4) was analyzed using an Agilent 490-PRO Micro-GC with Soprane II software, TCD detectors, and argon and helium carrier gas. The GC used two columns for separation, where column 1 was a 3m + 10m MS5A, RTS column with Ar carrier gas, and column 2 used a 10 m PPQ column with He carrier gas. In addition, LaserGas II and LaserDust instruments (NEO monitors) were used for measuring CO_2, O_2 and NO_x, as well as for dust analysis. Isokinetic sampling was performed on the off-gas for silica fume[25] and PAH analysis.

PAH Sampling Procedure. A sample collection system for PAH was developed by adapting a standard setup following isokinetic sampling principles to investigate PAH composition in gas and particle phase from the pilot furnace. A nozzle (4.16 mm) and probe (1/2 in., SS) were used to extract the gas from the off-gas duct. Glass fiber thimble filters (22 Ø, Munktell/Ahlstrom, Sweden), followed by cartridges with glass wool and XAD-2 (30.0 g, Supelpak-2, Merck Life Science AS, Germany), were used as absorbents. A rotary vane gas-sampler pump (Paul Gothe GmbH, Germany) was used to maintain stable gas flow. The setup is illustrated in Figure 2. By adjusting the

https://doi.org/10.1021/acs.iecr.2c04578
Ind. Eng. Chem. Res. XXXX, XXX, XXX−XXX

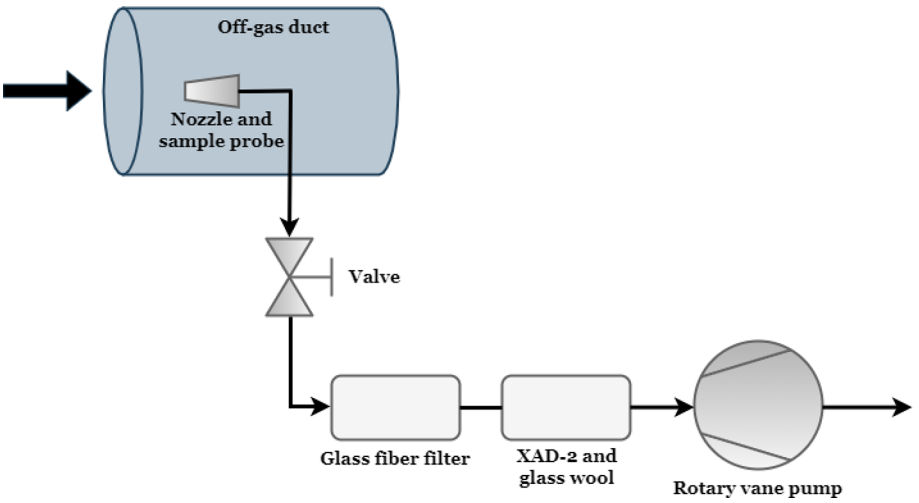

Figure 2. PAH sampling line, including glass fiber filter, XAD-2 cartridge with glass wool and rotary vane pump.

pump extraction velocity to match the gas flow in the off-gas duct, a representative sample extraction was achieved. After sample collection, the filters were removed and the filter holder was cleaned using acetone.

Samples for PAH analysis were obtained at specific experimental steps during the campaign, and process parameters are shown in Table 2. Samples were analyzed to investigate how the different process parameters affect concentration, molecular distribution and species of PAH. Glass fiber filters and XAD-2 cartridges were removed before tapping of Si metal. Sampling started when stable furnace conditions were reached, such as at target FGR ratio, off-gas concentration levels, and acceptable temperatures for the bag-house filter, and ended before tapping of the metal. On average, 0.30 Nm^3 off-gas was sampled per hour of silicon production. Sampling was performed at 14 different operation conditions, out of the 27 experimental cycles, and a total of 42 samples were collected (3 samples per experimental cycle). All samples were protected against UV radiation by layers of aluminum foil and stored at 4 °C in a dark location prior to analysis by Norwegian Institute of Air Research (NILU, Kjeller, Norway).

Table 2. Gas Flow, Recirculation Ratio and Oxygen Set-Points at PAH Sampling in the FGR Pilot Campaign

Sample Number	Flow [Nm^3/h]	FGR [%]	Oxygen [vol%]
1	1000	0	20.7
8	1000	0	20.7
14	1000	0	20.7
5	1000	70	17.2
11	1000	70	17.2
4	1000	88	10.0
13	1000	88	10.0
2	500	0	20.7
9	500	0	20.7
12	500	0	20.7
3	500	60	16.2
7	500	60	16.2
6	500	78	10.1
10	500	78	10.1

PAH Analysis Methodology. The analytical procedure follows the requirements of NILU's accreditation, according to NS-EN ISO/IEC 17025. Internal standards containing deuterated PAH congeners were added to all samples prior to extraction. Standards are listed in Table S2, found in the Supporting Information. XAD-2 and filter samples were Soxhlet extracted for 8 h in acetone/hexane (1:1), before the fraction was solvent exchanged to cyclohexane prior to liquid–liquid separation between cyclohexane and dimethyl formamide/water (Grimmer method), followed by cleanup using silica gel deactivated with 8% water (adsorption chromatography). After concentration, a recovery standard containing deuterated PAH congeners was added. Acetone samples were treated following the same method, without the Soxhlet extraction and solvent exchange to cyclohexane.

Identification and quantification of native PAHs was carried out using a gas chromatograph coupled to a low-resolution mass spectrometer as detector (GC/LRMS). The analyses were performed in EI mode using SIM. The list of PAH components is shown in Table 3.

Modeling PAH Evolution. A realistic model of the pilot scale submerged arc furnace is extremely complex due to the large uncertainty in the input data needed (like the types and amounts of PAH contained in the carbon materials in the furnace) apart from the transient nature of the flow. Additionally, the computational overhead to simulate such a process is not practical due to the large number of species and reactions that needs to be treated for PAH evolution along with the millions of cells required to mesh a furnace. To gain insight into the PAH evolution in such a complex system, a simplified geometry of a coflow burner is used in this work. The geometry is axisymmetric with a central fuel nozzle of radius equal to around 4 mm. The annulus through which flue gases are added has an inner radius of 4.5 mm and an outer radius of 180 mm, and the radius of the domain is equal to the outer radius of the annulus for the first 20 mm after which it increases to 190 mm for the next 1 m. The flue gases and the fuel are physically separated for the first 20 mm, after which the gases mix and react.

In the present study, only chemistry driven PAH is considered, and the work assumes that the fuel consists of C_2H_2, N_2 and H_2 and that these species are mainly responsible for the chemistry driven PAH.[22] This simplification is mainly

https://doi.org/10.1021/acs.iecr.2c04578
Ind. Eng. Chem. Res. XXXX, XXX, XXX−XXX

Table 3. List of 42 PAH Components Analyzed in the FGR Off-gas Samples

Compound	MW[g/mol]	T_b[a] [°C]	# of rings
Naphthalene	128.1	218	2
2-Methylnaphthalene	142.2	241	2
1-Methylnaphthalene	142.2	245	2
Biphenyl	154.2	255	2
Acenaphthylene	152.2	279	3
Acenaphthene	152.2	279	3
Dibenzofuran	168.2		3
Fluorene	166.2	294	3
Dibenzothiophene	184.3		3
Phenanthrene	178.2	338	3
Anthracene	178.2	340	3
3-Methylphenanthrene	192.3	352	3
2-Methylphenanthrene	192.3	355	3
2-Methylanthracene	192.3	359	3
9-Methylphenanthrene	192.3	355	3
1-Methylphenanthrene	192.3	359	3
Retene	234.3		3
Fluoranthene	202.3	383	4
Pyrene	202.3	393	4
Benzo(*a*)fluorene	216.3	407	4
Benzo(*b*)fluorene	216.3	402	4
Benz(*a*)anthracene	228.3	435	4
Triphenylene	228.3	439	4
Chrysene	228.3	448	4
Benzo(*ghi*)fluoranthene	226.3	432	5
Cyclopenta(*cd*)pyrene	226.3		5
Benzo(*b*)fluoranthene	252.3	481	5
Benzo(*k*)fluoranthene	252.3	481	5
Benzo(*j*)fluoranthene	252.3	480	5
Benzo(*a*)fluoranthene	252.3		5
Benzo(*e*)pyrene	252.3	493	5
Benzo(*a*)pyrene	252.3	496	5
Perylene	252.3		5
Dibenzo(*ac*)anthracene	278.3		5
Dibenzo(*ah*)anthracene	278.3		5
Indeno(1,2,3-*cd*)pyrene	276.3	536	6
Benzo(*ghi*)perylene	276.3	550	6
Anthanthrene	276.3		6
Coronene	300.4	430	6
Dibenzo(*ae*)pyrene	302.4	414	6
Dibenzo(*ai*)pyrene	302.4		6
Dibenzo(*ah*)pyrene	302.4		6

[a]PAH boiling point sources.[26,27]

due to the uncertainty in the type and amount of aromatic species bound to the carbon materials which, if they were known, could be used as fuel instead of the composition used in this work. Additionally, acetylene is reported in literature to be an important species for PAH growth, via HACA (hydrogen abstraction and acetylene or carbon addition mechanism, which involves repetitive abstraction of hydrogen from the aromatic species and addition of acetylene to the radical site) and soot evolution; see Reizer et al.[21] In this study, modeling is aimed at understanding the impact of flue gas recycling on PAH evolution from combustion of a mixture of acetylene (an aliphatic species) and hydrogen and comparing modeling outcomes with PAH emission observed in the furnace experiments. These gases are injected at 42.2 m/s at a constant temperature of 1000 °C with mass fractions (Y) of C_2H_2, N_2, and H_2 equal to 0.246, 0.708, and 0.046, respectively. The flue gases are assumed to consist (by mass fraction) of N_2 and Ar equal to 0.763 and 0.005 (note that the values are rounded to the third decimal), the mass fraction of O_2 is varied (the values used are 0.232, 0.203, 0.174, 0.145, 0.116 and 0.058), and the remaining fraction is CO_2. The decreasing O_2 content indicates higher levels of FGR. The flue gases are injected at 0.3 m/s at a constant temperature of 300 K. The walls separating the fuel and flue gases for the first 20 mm are set as no-slip walls, the top boundary is set as the outlet, and the remaining wall boundaries are assigned a fixed velocity of 0.3 m/s along the axial direction. The turbulence intensities of the inflow of fuel and coflow of flue gases/air are 8% and 2%, respectively, whereas turbulent mixing length scales (for both boundaries) are set to a value of 0.005 m.

The solver used to simulate the process is reactingFoam, a turbulent reacting flow solver available in the open source CFD framework OpenFOAM that does not treat buoyancy.[28] The solver accounts for conservation equations of mass, momentum, energy and species transport with treatment for species generation/consumption as well as heat released/consumed due to chemical reactions; see works in the literature[29] and S3 in the Supporting Information for details on the governing equations. The reaction kinetics and thermodynamic data for combustion including PAH evolution proposed by Slavinskaya et al.[22] were used in this work. It should be noted that there are more complex reaction mechanisms, which include soot evolution, that are reported in the literature to describe PAH evolution.[30,31] Since the experimental work analyzed PAH species with 2−6 rings, the reaction mechanism proposed by Slavinskaya et al.[22] is used in the model as it considers PAH up to the five ringed species (like benzo(*a*)pyrene). The reaction mechanism used in this work is based on acetylene combustion comprising 112 species and 939 reactions. It should be pointed out that this reaction mechanism does not distinguish between PAH species with the same chemical composition. The transport of gas species is assumed to be turbulence driven, so the species specific molecular/dynamic viscosity is calculated based on the Sutherland model with coefficients set to a constant value for all species (Sutherland coefficient equal to 1.512×10^{-6} kg/m·s and Sutherland temperature equal to 120 K). The combustion is treated using the Eddy Dissipation Concept (v2005) with turbulence treated using the standard $k-\epsilon$ model. The geometry used for the simulations is meshed using 18226 cells based on grid sensitivity studies, and the solver is run until a pseudo-steady state is reached.

RESULTS

Each experimental run lasted about 1.5 h and established the time frame for the test of one set of experimental parameters. An example of how the temperature varies within a cycle is shown in Figure 3. The cycle has a startup period and an end, which are not included when the average process parameters are calculated. At the start of a cycle, the system took some time to stabilize and reach set points for the experiment, and at the end of a cycle, the raw material charge would collapse, causing a blowout, and cause the process parameters to change. A more detailed description of variations within the experiments can be found in the work of Andersen et al.[25]

Flue gas recycling ratios, gas concentrations and flow values were calculated as an average over the stable sampling period. FGR is based on the ratio of inlet and outlet CO_2 concentration measurements by the NEO laser, and ambient

https://doi.org/10.1021/acs.iecr.2c04578
Ind. Eng. Chem. Res. XXXX, XXX, XXX−XXX

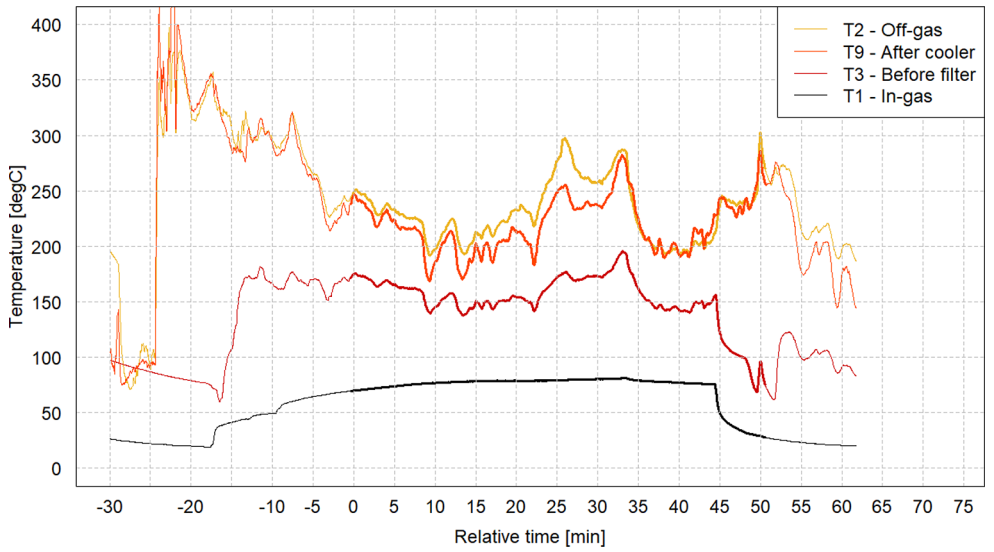

Figure 3. Example of temperature data for one experimental run. Temperature is logged for the off-gas, after the cooler, before the filter, and the inlet gas. The sampling period is highlighted, from 0 to 51 min.

CO_2 was set to 0.06 vol%. The measured flow, FGR and oxygen levels for each PAH sample are presented in Table 4.

Table 4. Measured Gas Flow, Recirculation Ratio and Oxygen Averages from PAH Sampling in the FGR Pilot Campaign, Sorted by Flow and Decreasing Oxygen Levels

Sample Number	Flow [Nm^3/h]	FGR [%]	Oxygen [vol %]	Flue Gas Temperature [°C]
1	965	0.6	20.7	208.3
8	914	0.9	20.7	248.6
5	935	60.1	17.6	238.1
4	865	81.3	15.5	231.7
13	919	82.5	13.3	237.1
9	566	0.3	20.4	268.4
3	440	56.6	17.9	275.3
7	497	59.6	17.3	292.9
6	425	75.0	16.4	274.7

After evaluation, results from four tapping cycles were deemed to be unreliable, as no PM was collected in the glass fiber filters even though the sampling pump registered gas flow, indicating a leak in the sampling line with only ambient air being sampled. Results from sample number 2 were determined to be an outlier, as comparing with experiments of similar FGR (0−1%); the result did not fit within a 90% confidence interval.

PAH Emissions during Si Production. Three experiments were performed as conventional Si production cycles, without flue gas recirculation (samples 1, 8 and 9). One experiment had a gas flow rate at 500 Nm^3/h and two had flow rates of 1000 Nm^3/h. The total PAH-42 concentrations for these experiments range between 14.1 and 22.0 $\mu g/Nm^3$. To compare, the PAH EPA-16 concentration range is between 8.5 and 12.9 $\mu g/Nm^3$ for the same experiments.

Effect of FGR on Flue Gas Composition. Figure 4(a−d) shows how O_2, temperature, CO and CH_4 changes with the level of FGR during the pilot experiments. The FGR levels vary from 0 to 75.0% for experiments at 500 Nm^3/h and from 0 to 82.5% for experiments at 1000 Nm^3/h (Table 4). Figure 4(a) shows the change in O_2 as an effect of FGR, and similar decreasing trends are present for both 500 and 1000 Nm^3/h, with a significant drop in O_2 concentration occurring at 80% FGR for the 1000 Nm^3/h set point. This is also illustrated in panel (c), where the changes in CO levels at 1000 Nm^3/h increase from about 500 to 700 ppm when the FGR increases from 81.3 to 82.5%, respectively. The off-gas temperature was measured before the cooler (Figure 1), and the average values are presented in Figure 4(b). All temperature measurements at 500 Nm^3/h were at a higher level than for 1000 Nm^3/h. Often, the operations were limited by the operational conditions for the bag-house filter (at 185 °C) and were often adjusted by directing gas through the smokestack at the beginning of a cycle and delaying the start of the sampling while waiting for the temperature to stabilize. The levels of methane shown in panel (d) display no significant changes with the varying FGR ratios and oxygen at the experimental steps where PAH were sampled.

Effect of FGR and O_2 Levels on PAH Emissions. Figure 5 shows how the total concentration of PAH-42 changes with varying (a) FGR ratios and (b) oxygen levels for samples at 1000 and 500 Nm^3/h. At 1000 Nm^3/h, the PAH concentration increases from 16.0 to 559.7 $\mu g/Nm^3$ with decreasing O_2 levels (20.7−13.3 vol %) and increasing FGR (0−82.5%). Overall, the PAH concentrations are lower for the samples at 500 Nm^3/h conditions than at 1000 Nm^3/h, ranging between 22.0 and 107.8 $\mu g/Nm^3$, when comparing with similar FGR (0−75.0%) and oxygen levels (20.4−16.4 vol %).

A correlation was found between the total PAH-42 concentration and the level of oxygen and FGR, at 99.0% and 89% confidence, respectively. By separating the PAH into fractions of LMW and HMW, the correlation was found to be at a 96.0% confidence interval between LMW PAHs and the level of oxygen and 76.0% for FGR and, as well as a 99.0% and 97.0% confidence interval between HMW PAHs and oxygen and FGR, respectively.

Each experiment produced three samples from the sampling line. PAH contents were analyzed from the filter, acetone washing liquid and XAD-2 absorbent. The normalized distribution of total PAH concentration between the elements in the sampling line is presented in Figure 6 for all experiments. The majority of the PAH species are caught in the glass fiber filter. For experiments at 0% FGR, 57% of the

https://doi.org/10.1021/acs.iecr.2c04578
Ind. Eng. Chem. Res. XXXX, XXX, XXX−XXX

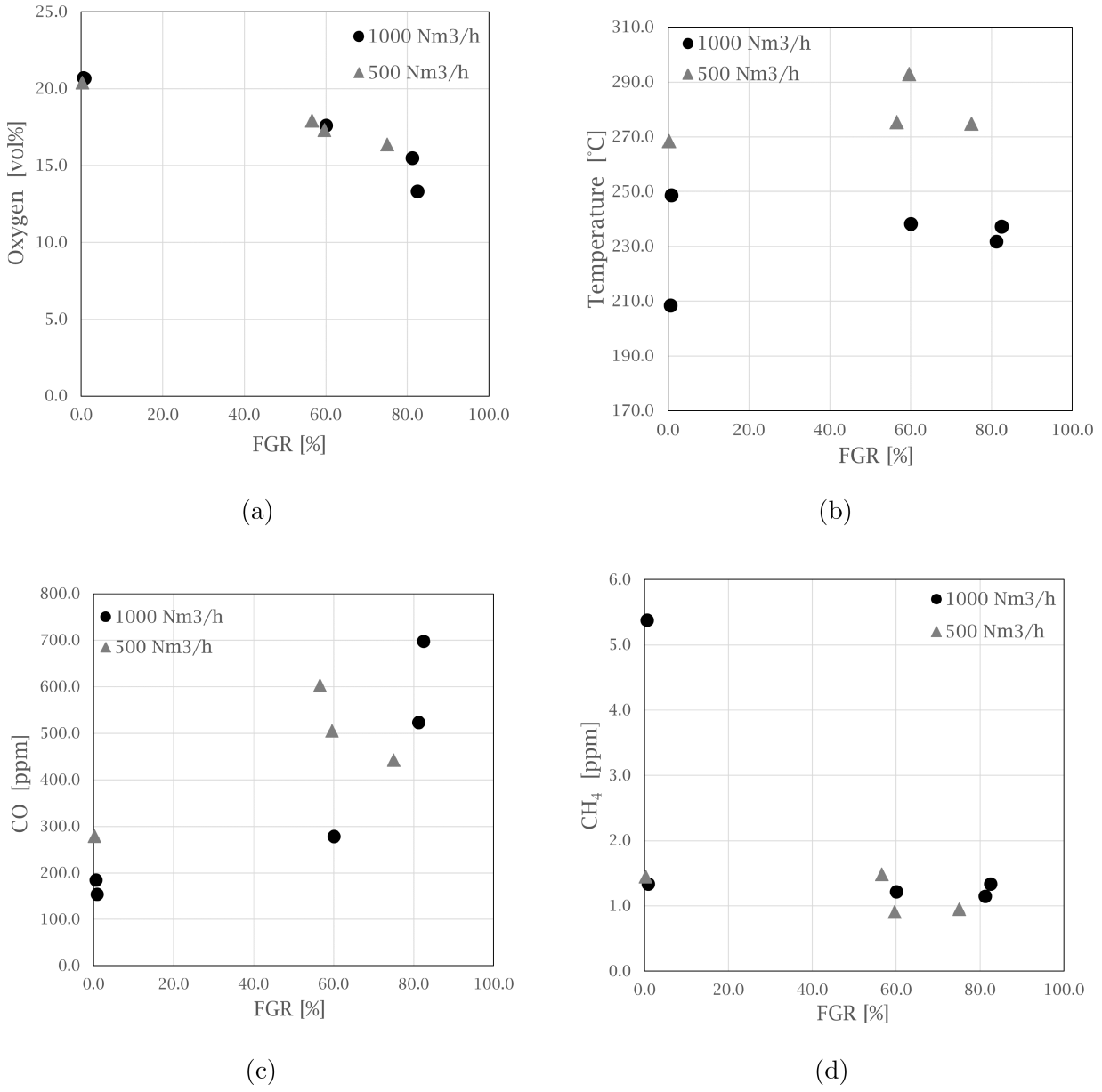

Figure 4. Graphs showing the changes in gas composition and temperature as an effect of FGR for the different flow rates (500 and 1000 Nm^3/h): (a) O_2, (b) temperature, (c), CO, and (d) CH_4.

average amount of the total PAHs was found in the filter. In this fraction, the 4−6 ring high molecular weight (HMW) PAH makes up 71%, and the remaining 29% is the light molecular weight (LMW) PAH with 2 and 3 rings. The experiment at 82.5% FGR is notable, at 1000 Nm^3/h as shown in 6(a), where 77.7% of the PAH passed through the filter and 67.5% were of LMW.

Diagnostic Ratios. As shown in Figure 7, the generally dominating ratio is the fraction of high molecular weight with 4−6 ring PAHs for both 1000 and 500 Nm^3/h experiments, with a pyrogenic ratio of LMW/HMW < 1, and it does not seem to be greatly affected by the FGR rate. This is also supported by the cross-plot in Figure 8, where the ratios of Phen/Anth and Fla/Py show that all of the experiments are placed within the pyrogenic area.

The experiment at 82.5% FGR and 1000 Nm^3/h stands out. Compared with the ratios shown in Figure 6, the PAH levels for this experiment mainly consist of gaseous naphthalene absorbed on XAD-2, which shifts the LMW/HMW ratio from below or close to 1 to above 1 and toward a petrogenic diagnostic ratio.

PAH EPA-16 and PAH-42. In Figure 9 a comparison between PAH EPA-16 and the 42 PAH components analyzed is shown. The comparison shows that the PAH-16 makes up on average 62% and 58% of the total PAHs for experiments at 1000 and 500 Nm^3/h, respectively. The ratio is stable and is not seemingly affected by the combustion conditions in the furnace and the FGR levels.

PAH Evolution with FGR in the Simplified Simulations. The increase in the flue gas recirculation is observed to decrease temperature as expected, but low oxygen levels in the flue gas (corresponding to mass fraction based % equal to 11.6% and 5.8%) result in no combustion despite the occurrence of some reactions (forming PAHs and water), as seen in Figure 10 and Figure 11. In the simulation where combustion occurs (i.e., mass fraction based oxygen % of

https://doi.org/10.1021/acs.iecr.2c04578
Ind. Eng. Chem. Res. XXXX, XXX, XXX−XXX

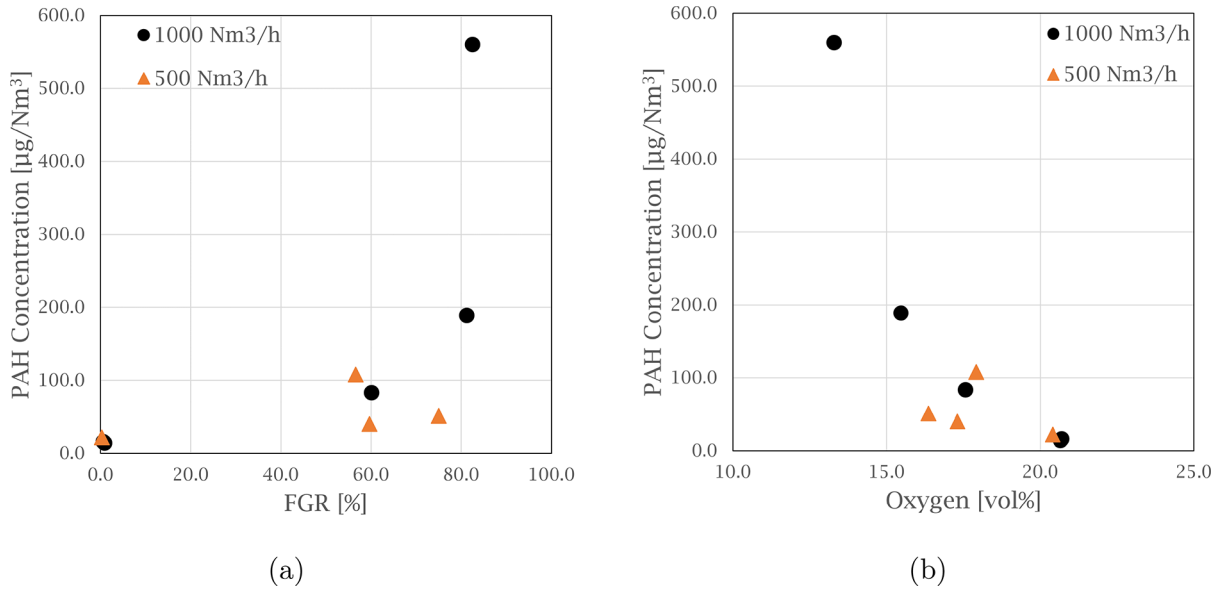

Figure 5. Graphs showing the total PAH-42 concentration in the off-gas at varying (a) FGR ratios and (b) O_2 levels for experiments at 1000 and 500 Nm^3/h.

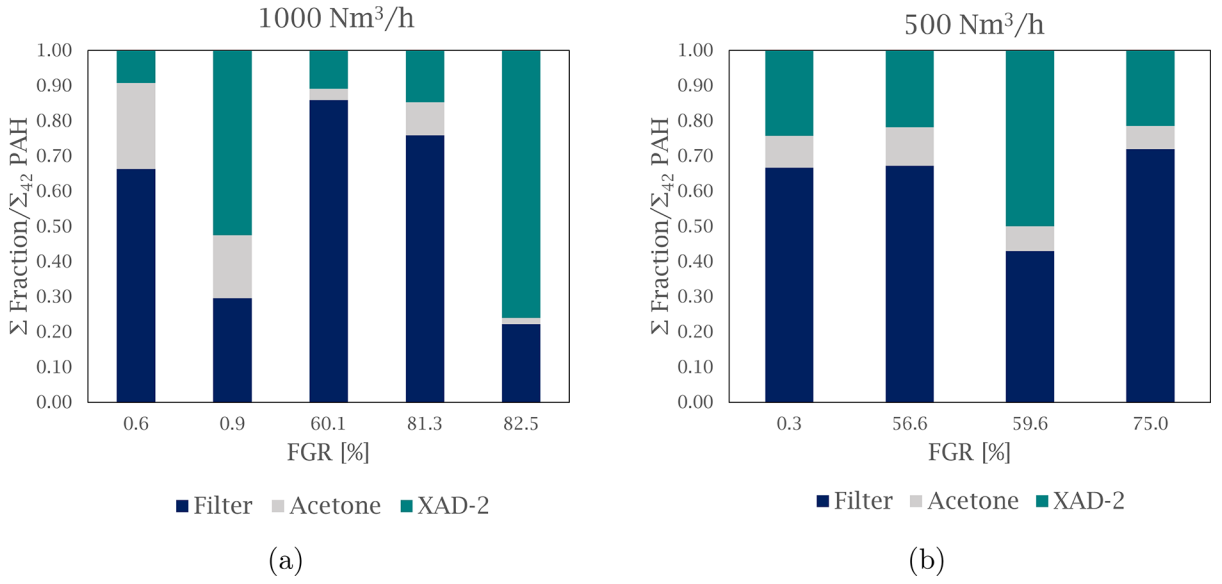

Figure 6. Graphs showing the normalized distribution of PAHs between the filter, washing liquid (acetone), and XAD-2, at varying FGR: (a) experiments at 1000 Nm^3/h and (b) experiments at 500 Nm^3/h.

23.2−14.5%), the PAH generated is observed to get oxidized as these species are convected through the flame front or the region with the high temperature. In the cases with no combustion and FGR with mass fraction based O_2 % of 11.6% and 5.8%, the PAHs generated are transported all the way to the outlet as they never encounter high enough temperature for oxidization. These simulations indicate that the oxidation process of PAH species is dependent on the locally available oxygen, temperature and residence time.

To study the conditions that prevent the oxidation of PAHs, a perfectly stirred reactor (PSR) simulation (see Meeks et al.[32] and S4 in the Supporting Information for further details on the reactor model), in which a mixture of PAH (i.e., A1 or benzene), O_2, CO_2 and N_2 reacts in a 0D reactor at constant temperature until reaching equilibrium, is used. The results from the PSR simulations (see Figure 12) suggest that temperatures below 1000 K, with residence time smaller than 1 s, and low oxygen can prevent the complete oxidation of benzene.

The PSR simulations show that the main product at equilibrium is carbon dioxide, indicating that oxidization of the benzene is more dominant when compared to benzene's growth into larger PAH species. The composition of larger PAH species at equilibrium predicted by the PSR simulation shows a dependence on temperature, residence time and oxygen levels. So at sufficiently high temperatures (around 1500 K) benzene is observed to be oxidized completely, but at lower temperatures it can partly be oxidized and grow into larger PAHs. If the PAH species are not oxidized, it can evolve into larger/smaller PAH molecules based on the local flow conditions as well as be transported to the off-gas duct of the furnace.

https://doi.org/10.1021/acs.iecr.2c04578
Ind. Eng. Chem. Res. XXXX, XXX, XXX−XXX

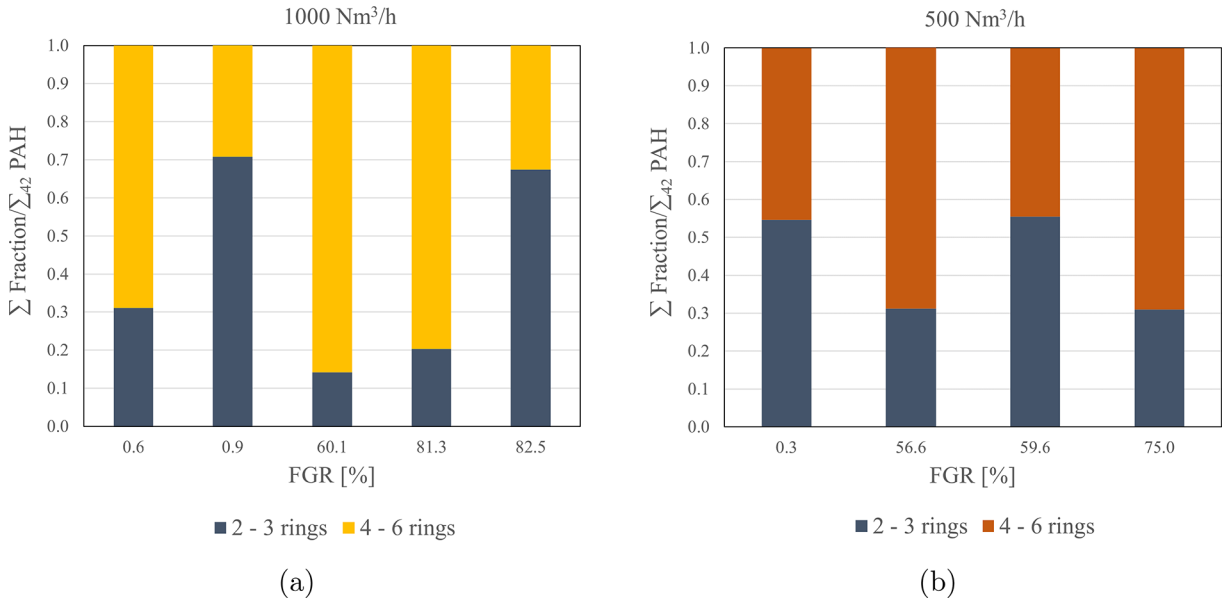

Figure 7. Graphs showing distribution between low molecular weight (2−3 rings) PAHs and high molecular weight (4−6 rings) PAHs in the off-gas at varying FGR: (a) experiments at 1000 Nm^3/h and (b) experiments at 500 Nm^3/h.

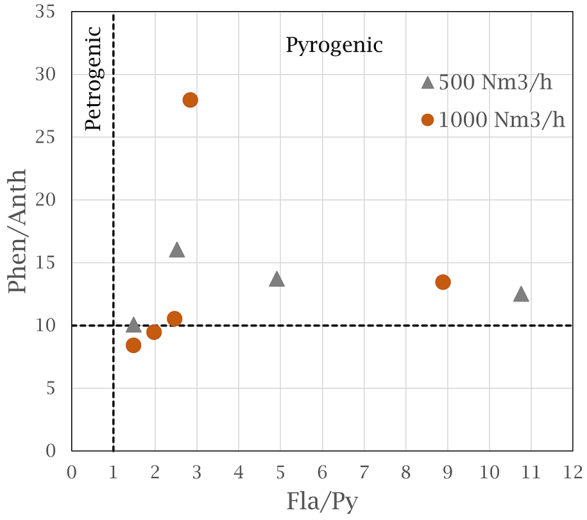

Figure 8. Cross-plot of Phen/Anth and Fla/Py ratios for all experiments in the FGR Si pilot campaign. Lines at $x = 1$ and $y = 10$ suggest the separation of petrogenic and pyrogenic sources for the two ratios, as suggested by Budzinski et al.[7]

As the PAH is oxidized in the simulations with combustion, potential PAH emission from the various scenarios simulated can be understood by simply comparing the maximum mass fraction value of a PAH species in the domain predicted by the model. The maximum amounts of various aromatic species produced for the various flue gas recycling cases are visualized in Figure 13. The reduction in oxygen with increased FGR is generally observed to increase the generation of the aromatic species. The simulations predict that although no combustion is observed in FGR with mass fraction based O_2 % of 11.6% and 5.8%, PAH species formed (especially A1 and A2) are approximately in the same order of magnitude as the other FGR cases. The maximum value of A2 or naphthalene is found to increase up to FGR with a mass fraction based O_2 % of 11.6%. The subsequent increase in FGR is observed to result in a reduction of A2. Comparing the maximum value of the PAH species formed, smaller PAH species like A1 and A2 tend to be formed in larger amounts when compared to the larger aromatic species (except for BAPYR, which could be due to overestimation as the reaction mechanism does not consider even larger PAH species).

DISCUSSION

The three experiments from Si production without FGR have a PAH-42 concentration between 14.1 and 22.0 $\mu g/Nm^3$. Comparing these experiments with the emission levels reported by Gaertner et al.[13] of 2 $\mu g/Nm^3$, and taking into account the sampling location of Gaertner being after the bag-house filter, which would contribute to decreasing emissions, the results are within a similar range. Sampling by Gaertner was performed during a furnace start-up, and it was noted that the PAH profile changed from bicyclic to heavier compounds, such as phenanthrene and fluoranthene, over time.

At 1000 Nm^3/h, the PAH concentration increased from 16.0 to 559.7 $\mu g/Nm^3$ with decreasing O_2 levels (20.7−13.3 vol %) and increasing FGR (0−82.5%), which are parameters that show a strong correlation in this study. This follows the trend presented in other work where the level of unburned hydrocarbons increased with increasing levels of FGR.[18,19] This overall trend, also observed in modeling, is a consequence of the lower availability of oxygen and the reduction in temperature, due to which the extent of oxidation of the PAH is reduced. All eight modeled aromatic species showed a steady increase in concentration, with A1 and A2 (benzene and naphthalene) being the dominating species. This is also observed in the pilot experiment with increasing concentration of naphthalene at low oxygen levels (13.3 vol %). It should also be noted that at very high levels of FGR, the combustion in the furnace hood can also potentially be hindered depending on the flammability limit of SiO and CO gases, similar to the lack of combustion observed in the CFD simulation using FGR with mass fraction based O_2 % of 11.6% and 5.8%. With added FGR, PAH that passes through the bag-house filter could recirculate back to the furnace hood and be oxidized and continue back in the loop as CO_2 or a different PAH (or

https://doi.org/10.1021/acs.iecr.2c04578
Ind. Eng. Chem. Res. XXXX, XXX, XXX−XXX

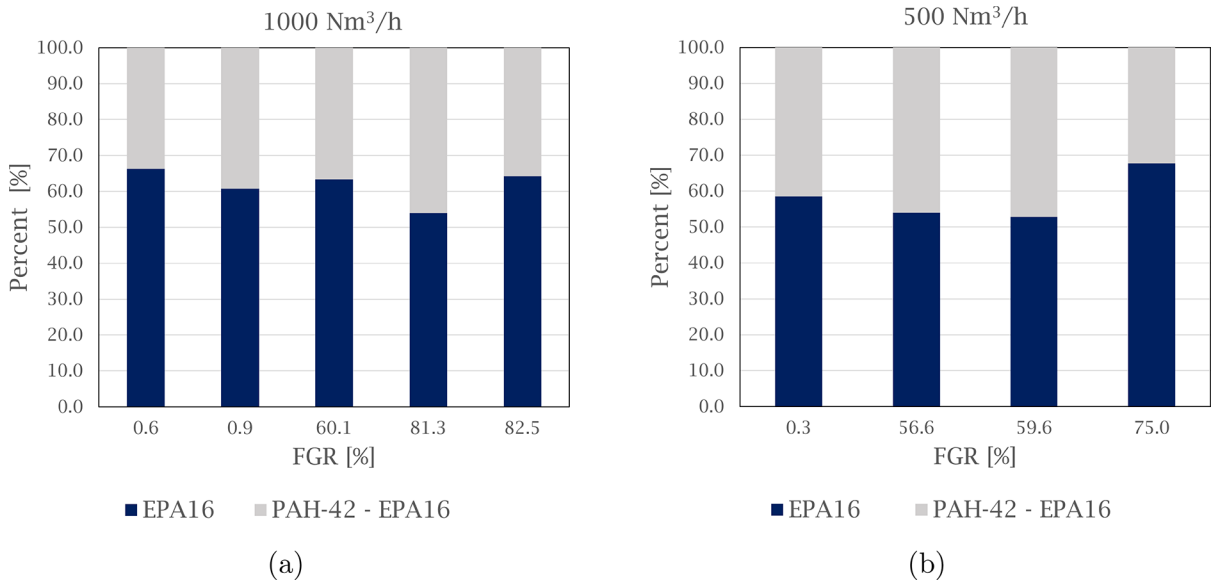

Figure 9. Graphs showing percent distribution between PAH EPA-16 and PAH-42 for all experiments at varying FGR: (a) experiments at 1000 Nm^3/h and (b) experiments at 500 Nm^3/h.

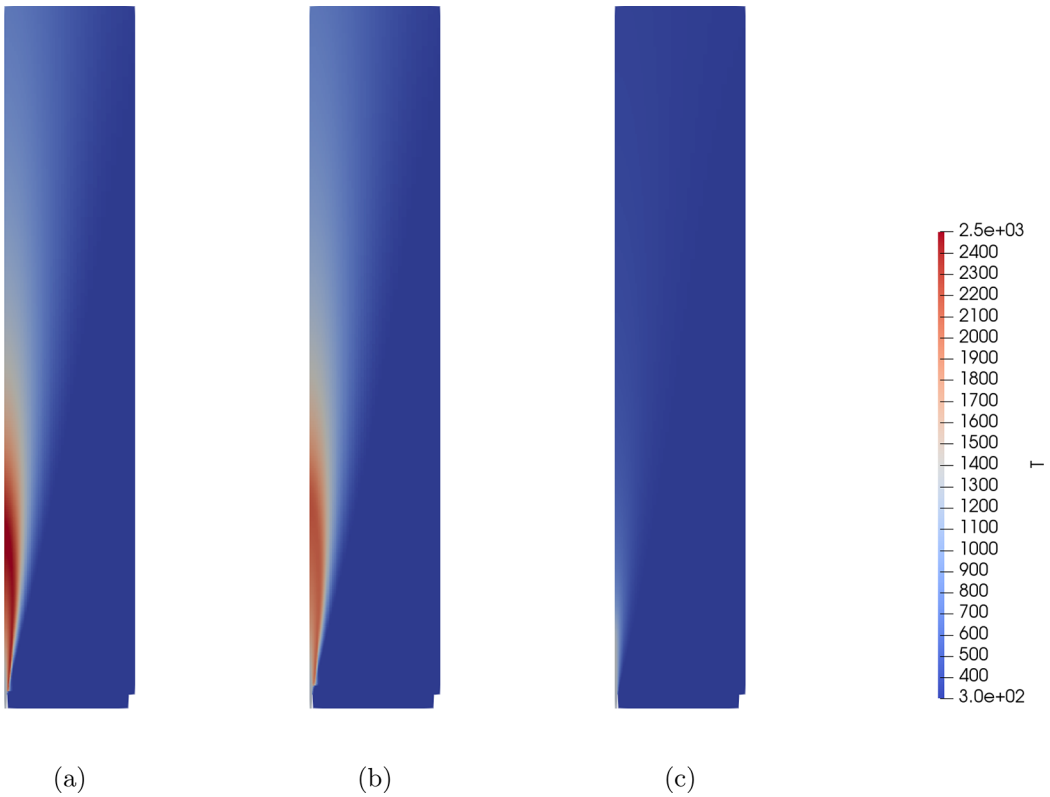

Figure 10. Contour plots of temperature (in K) distribution for varying levels of FGR or O_2 (mass fraction based %) in flue gas: (a) 23.2%, (b) 17.4%, and (c) 11.6%.

hydrocarbon species), or could pass through the combustion zone and increase in concentration if new PAHs are formed in the Si furnace. It should be noted that the CFD simulations in this work assumed that the flue gases are always injected at a constant temperature of 300 K without any PAH, which may not occur in the experiment as the flue gas temperature is often higher than the surrounding air and may contain some PAH species. Numerical modeling to study the impact of PAH in the recirculated flue gases and at temperatures higher than 300 K should be investigated in future works.

All temperature measurements at 500 Nm^3/h were at a higher level than for 1000 Nm^3/h, indicating that the temperature could be more affected by the volume of gas and the dilution of heat in a fuel rich environment than the direct effects of FGR. Liu et al.[20] observed increased combustion efficiency of C_2H_4 in a fuel rich flame at elevated temperatures with exhaust gas recirculation (EGR) when

https://doi.org/10.1021/acs.iecr.2c04578
Ind. Eng. Chem. Res. XXXX, XXX, XXX−XXX

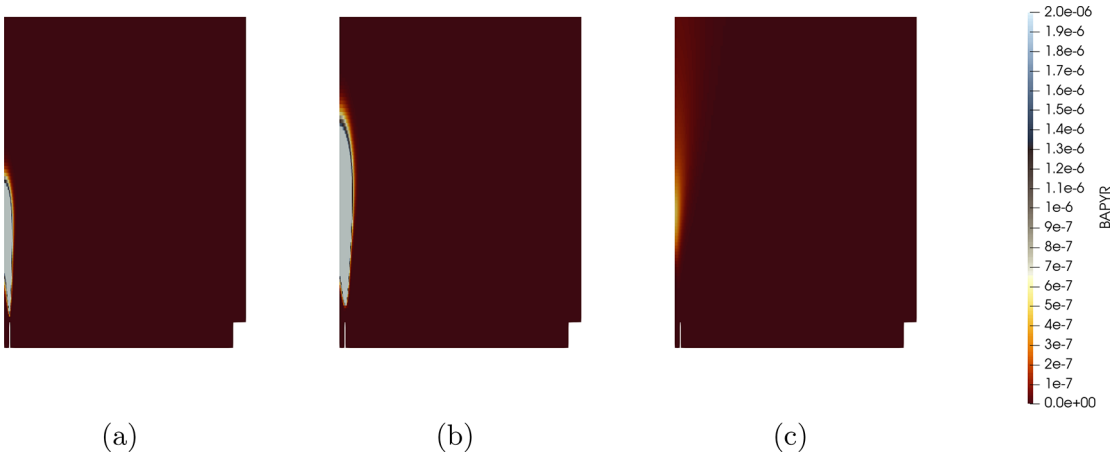

Figure 11. Zoomed-in contour plots of mass fraction of BAPYR ($C_{20}H_{12}$ or benzo(*a*)pyrene) distribution for varying levels of FGR or O_2 (mass fraction based %) in flue gas: (a) 23.2%, (b) 17.4%, and (c) 11.6%.

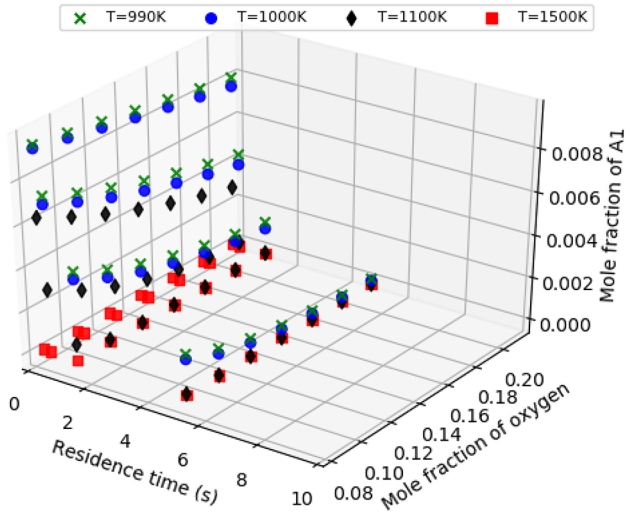

Figure 12. Predicted mole fraction of A1 (or benzene) at equilibrium that did not get oxidized based on PSR simulation. The simulation is run at 1 atm, constant temperature (which is varied as shown in the legend), and mole fractions of N_2 and A1 set to constant values equal to 0.78 and 0.01; the mole fraction of O_2 is varied (on the *y*-axis), and the remainder is assumed to be CO_2.

studying PAH formation, which could be the explanation for the lower PAH concentrations at lower flow rates. As lower flow of flue gases is observed to increase the temperature in the furnace during experiments, this may increase the overall residence time experienced by PAH species, thus increasing the extent of oxidation of PAH species as observed in Figure 12. It should also be noted that the PSR simulations also indicate that the complete oxidation of A1 or benzene can be prevented if the residence time is lower than 1 s, which agrees roughly with the conclusion of Panjwani et al.,[23] who recommended a residence time larger than 2 s for complete oxidation of 1-methylnaphthalene. Despite lower emission levels in general at lower flow, the HMW fraction dominates the emission profile together with production of the more thermodynamically stable species of phenanthrene and fluoranthene, suggesting that the process remain at high temperature oxidative conditions even at the extreme process conditions tested in the pilot campaign.

To be able to simulate scenarios comparable to experiments, the composition of the process gases emitted from the charge surface needs to be understood well as these gases are assumed to consist of just SiO and CO and details on the in-furnace formed PAH are not known. Another important direction for future investigation is to include PAH species larger than five rings, using an even more detailed reaction mechanism, like the mechanism proposed by Pejpichestakul et al.[31] that treats soot evolution and has around 25000 reactions involving approximately 400 species. Inclusion of larger PAH and soot into the model could aid in accurately capturing the evolution of PAH as the aromatic species considered in this work were observed to get oxidized (see Figure 11), whereas in experiments involving similar flame emission of soot and PAH have been reported.[33] Despite the simplifications in the modeling performed in this work, the overall trends obtained support the experimental observations, indicating the ability of the model to describe complex reactive flow phenomena occurring in the furnace hood.

CONCLUSIONS

The influence of FGR on PAH emissions was investigated in this study, through both experimental testing and CFD modeling. The PAH emissions were measured during Si alloy production in a pilot scale furnace with FGR and various levels of O_2 and flue gas flow.

- The concentration of PAH-42 for experiments with no FGR varied between 14.1 and 22.0 $\mu g/Nm^3$. With increasing recycling rate of furnace gas and decreasing O_2 levels, the concentration of PAH increased, independent of the flue gas flow. The PAH-42 concentration increased up to 559.7 $\mu g/Nm^3$, with 13.3 vol % O_2 at 1000 Nm^3/h. A correlation was found between the total PAH-42 concentration and the level of oxygen and FGR, at 99.0% and 89% confidence, respectively.
- High molecular weight PAHs dominated the PAH profile in the experimental samples and made up on average 58% of the total sample. A noticeable shift was observed at low oxygen levels and high FGR, where bicyclic PAHs, such as naphthalene, made up increasing levels of the total sample. Diagnostic ratios suggest the emission profiles fit a pyrogenic high temperature oxidative process, which promotes thermodynamically stable PAH species.
- Simulations showed that an increased level of FGR (without any recycling of PAH) could result in larger amounts

https://doi.org/10.1021/acs.iecr.2c04578
Ind. Eng. Chem. Res. XXXX, XXX, XXX−XXX

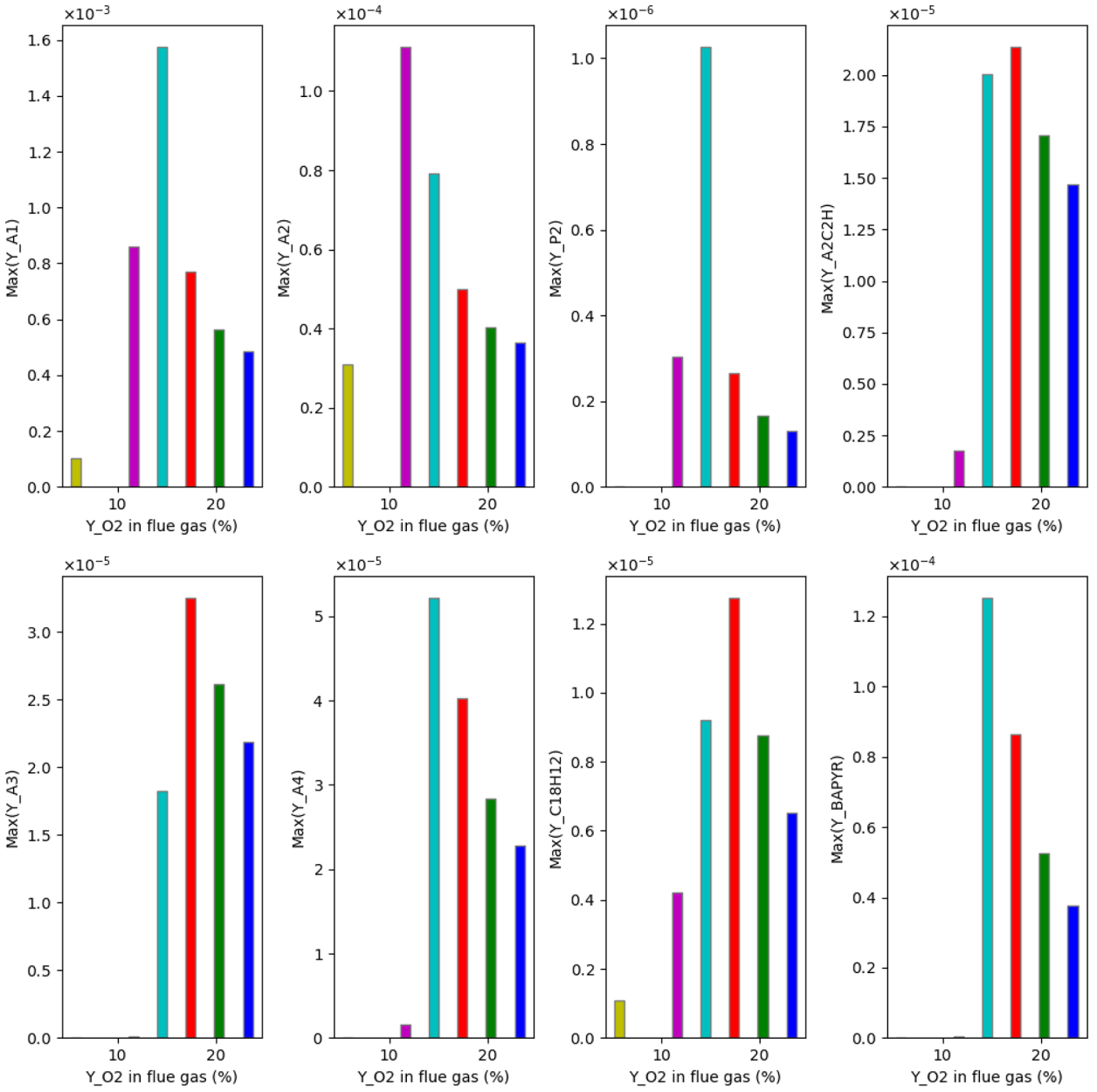

Figure 13. Comparison of the maximum value of mass fraction of 8 aromatic species predicted by the CFD simulations for various flue gas recycling scenarios. The *x*-axis of the plots represents O_2 (mass fraction based %) in the injected flue gas calculated as the mass fraction of $O_2 \times 100$. These 8 aromatic species are A1 (C_6H_6 or benzene), A2 ($C_{10}H_8$ or naphthalene), P2 ($C_{12}H_{10}$ or acenaphthene), A2C2H ($C_{12}H_8$ or acenaphthylene), A3 ($C_{14}H_{10}$ or anthracene/phenanthrene), A4 ($C_{16}H_{10}$ or fluoranthene/pyrene), C18H12 ($C_{18}H_{12}$ or benzo(*a*)anthracene/chrysene), and BAPYR ($C_{20}H_{12}$ or benzo(*a*)pyrene).

of PAH formed. The simulations predicted a propensity for formation of smaller aromatic species (like benzene and naphthalene) when compared to the larger PAH species with the exception of benzo(*a*)pyrene (BAPYR), which could be a result of the reaction mechanism treating PAH evolution until BAPYR.

- Investigation of the oxidation of PAH species (represented by benzene) showed that complete oxidation of benzene could be prevented with temperatures lower than 1000 K and residence times smaller than 1 s, while complete oxidation was found at temperatures of around 1500 K.

■ ASSOCIATED CONTENT

Supporting Information

The Supporting Information is available free of charge at https://pubs.acs.org/doi/10.1021/acs.iecr.2c04578.

Full overview of the PAH analysis results, list of the standards used for analysis, and information on the OpenFOAM solver and the perfectly stirred reactor model (PDF)

■ AUTHOR INFORMATION

Corresponding Authors

Kamilla Arnesen − *Department of Materials Science and Engineering, Norwegian University of Science and Technology*

https://doi.org/10.1021/acs.iecr.2c04578
Ind. Eng. Chem. Res. XXXX, XXX, XXX−XXX

(NTNU), 7034 Trondheim, Norway; orcid.org/0000-0003-2259-1334; Email: kamilla.arnesen@ntnu.no
Gabriella Tranell − *Department of Materials Science and Engineering, Norwegian University of Science and Technology (NTNU), 7034 Trondheim, Norway*; Email: gabriella.tranell@ntnu.no

Authors

Kurian J. Vachaparambil − *SINTEF Industry, 7034 Trondheim, Norway*
Vegar Andersen − *Department of Materials Science and Engineering, Norwegian University of Science and Technology (NTNU), 7034 Trondheim, Norway*; orcid.org/0000-0002-6486-0785
Balram Panjwani − *SINTEF Industry, 7034 Trondheim, Norway*; orcid.org/0000-0002-9700-2672
Katarina Jakovljevic − *Department of Materials Science and Engineering, Norwegian University of Science and Technology (NTNU), 7034 Trondheim, Norway*
Ellen Katrin Enge − *Norwegian Institute of Air Research (NILU), 2007 Kjeller, Norway*
Heiko Gaertner − *SINTEF Industry, 7034 Trondheim, Norway*
Thor Anders Aarhaug − *SINTEF Industry, 7034 Trondheim, Norway*
Kristian Etienne Einarsrud − *Department of Materials Science and Engineering, Norwegian University of Science and Technology (NTNU), 7034 Trondheim, Norway*

Complete contact information is available at: https://pubs.acs.org/10.1021/acs.iecr.2c04578

Notes

The authors declare no competing financial interest.

■ ACKNOWLEDGMENTS

This work was funded by the Norwegian Research Council and the Center for Research-based Innovation, SFI Metal Production (NFR Project number 237738) as well as FME HighEFF (Project number 257632).

■ REFERENCES

(1) Abdel-Shafy, H. I.; Mansour, M. S. M. A review on polycyclic aromatic hydrocarbons: Source, environmental impact, effect on human health and remediation. *Egyptian Journal of Petroleum* **2016**, *25*, 107−123.
(2) European Union, Decision No. 1386/2013/EU of the European Parliament and of the Council of 20 November 2013 on a General Union Environment Action Program to 2020 'Living well, within the limits of our planet'; 2013.
(3) Zhang, Y.; Tao, S. Global atmospheric emission inventory of polycyclic aromatic hydrocarbons (PAHs) for 2004. *Atmos. Environ.* **2009**, *43*, 812−819.
(4) Andersson, J. T.; Achten, C. Time to Say Goodbye to the 16 EPA PAHs? Toward an Up-to-Date Use of PACs for Environmental Purposes. *Polycyclic Aromatic Compounds* **2015**, *35*, 330−354.
(5) Lima, A. L. C.; Farrington, J. W.; Reddy, C. M. Combustion-Derived Polycyclic Aromatic Hydrocarbons in the Environment—A Review. *Environmental Forensics* **2005**, *6*, 109−131.
(6) Tobiszewski, M.; Namieśnik, J. PAH diagnostic ratios for the identification of pollution emission sources. *Environ. Pollut.* **2012**, *162*, 110−119.
(7) Budzinski, H.; Jones, I.; Bellocq, J.; Piérard, C.; Garrigues, P. Evaluation of sediment contamination by polycyclic aromatic hydrocarbons in the Gironde estuary. *Marine Chemistry* **1997**, *58*, 85−97.
(8) Pies, C.; Hoffmann, B.; Petrowsky, J.; Yang, Y.; Ternes, T. A.; Hofmann, T. Characterization and source identification of polycyclic aromatic hydrocarbons (PAHs) in river bank soils. *Chemosphere* **2008**, *72*, 1594−1601.
(9) Zhang, W.; Zhang, S.; Wan, C.; Yue, D.; Ye, Y.; Wang, X. Source diagnostics of polycyclic aromatic hydrocarbons in urban road runoff, dust, rain and canopy throughfall. *Environ. Pollut.* **2008**, *153*, 594−601.
(10) Schei, A.; Tuset, J.; Tveit, H. *Production of High Silicon Alloys*; Tapir: Trondheim, 1998.
(11) Kero, I.; Grådahl, S.; Tranell, G. Airborne Emissions from Si/FeSi Production. *JOM* **2017**, *69*, 365−380.
(12) Eidet, T.; Mikkelsen, Ø. PAH-free binders in metallurgical carbon pastes. The 15th International Ferroalloys Congress INFACON XV, Cape Town, 2018.
(13) Gaertner, H.; Aarhaug, T. A.; Wittgens, B.; Hunsbedt, L.; Legård, M.; Tranell, G. Measurements of PAH emissions in the ferro-alloy industry. The 15th International Ferroalloys Congress INFACON XV. Cape Town, 2018.
(14) Norwegian Environmental Agency, Norske utslipp - Utslipp til luft og vann og generert avfall, PAH-16-USEPA. https://www.norskeutslipp.no.
(15) Normann, F.; Skafestad, R.; Bierman, M.; Wolf, J.; Mathisen, A. Reducing the Cost of Carbon Capture in Process Industry. 2019; https://www.sintef.no.
(16) Mathisen, A.; Normann, F.; Biermann, M.; Skagestad, R.; Haug, A. T. *CO2 Capture Opportunities in the Norwegian Silicon Industry*; SINTEF Academic Press: 2019.
(17) Henningsen, S. In *Handbook of Air Pollution From Internal Combustion Engines*; Sher, E., Ed.; Academic Press: San Diego, 1998; pp 477−534.
(18) Chen, S.; Cui, K.; Zhu, J.; Zhao, Y.; Wang, L.-C.; Mutuku, J. K. Effect of Exhaust Gas Recirculation Rate on the Emissions of Persistent Organic Pollutants from a Diesel Engine. *Aerosol and Air Quality Research* **2019**, *19*, 812−819.
(19) Abdelaal, M.; El-Riedy, M.; El-Nahas, A. Effect of flue gas recirculation on burner performance and emissions. *Journal of Al-Azhar University Engineering Sector* **2016**, *11*, 1275−1284.
(20) Liu, P.; Zhang, Y.; Wang, L.; Tian, B.; Guan, B.; Han, D.; Huang, Z.; Lin, H. Chemical Mechanism of Exhaust Gas Recirculation on Polycyclic Aromatic Hydrocarbons Formation Based on Laser-Induced Fluorescence Measurement. *Energy Fuels* **2018**, *32*, 7112−7124.
(21) Reizer, E.; Viskolcz, B.; Fiser, B. Formation and growth mechanisms of polycyclic aromatic hydrocarbons: A mini-review. *Chemosphere* **2022**, *291*, 132793.
(22) Slavinskaya, N.; Mirzayeva, A.; Whitside, R.; Starke, J.; Abbasi, M.; Auyelkhankyzy, M.; Chernov, V. A modelling study of acetylene oxidation and pyrolysis. *Combust. Flame* **2019**, *210*, 25−42.
(23) Panjwani, B.; Andersson, S.; Wittgens, B.; Olsen, J. E. *Cleaning of polycyclic aromatic hydrocarbons (PAH) obtained from ferroalloys plant*; SINTEF Academic Press: 2017.
(24) Andersen, V.; Solheim, I.; Gaertner, H.; Sægrov-Sorte, B.; Einarsrud, K. E.; Tranell, G. In *REWAS 2022: Developing Tomorrow's Technical Cycles (Vol. I)*; The Minerals, Metals & Materials Series; Lazou, A., Daehn, K., Fleuriault, C., Gökelma, M., Olivetti, E., Meskers, C., Eds.; Springer International Publishing: Cham, 2022; pp 555−564.
(25) Andersen, V.; Solheim, I.; Gaertner, H.; Sægrov-Sorte, B.; Einarsrud, K. E.; Tranell, G. Pilot-Scale Test of Flue Gas Recirculation for The Silicon Process. *Journal of Sustainable Metallurgy* **2023**, *9*, 81−92.
(26) National Institute of Health. *PubChem*. 2022; https://pubchem.ncbi.nlm.nih.gov/ (accessed 2022−03−14).
(27) Bjørseth, A. *Handbook of polycyclic aromatic hydrocarbons*; Marcel Dekker: New York, 1983.
(28) Greenshields, C. *OpenFOAM v8 User Guide*; The OpenFOAM Foundation: London, U.K., 2020.

(29) Li, T.; Pan, J.; Kong, F.; Xu, B.; Wang, X. A quasi-direct numerical simulation solver for compressible reacting flows. *Computers & Fluids* **2020**, *213*, 104718.
(30) Richter, H.; Granata, S.; Green, W. H.; Howard, J. B. Detailed modeling of PAH and soot formation in a laminar premixed benzene/oxygen/argon low-pressure flame. *Proceedings of the Combustion Institute* **2005**, *30*, 1397−1405.
(31) Pejpichestakul, W.; Ranzi, E.; Pelucchi, M.; Frassoldati, A.; Cuoci, A.; Parente, A.; Faravelli, T. Examination of a soot model in premixed laminar flames at fuel-rich conditions. *Proceedings of the Combustion Institute* **2019**, *37*, 1013−1021.
(32) Meeks, E.; Grcar, J. F.; Kee, R. J.; Moffat, H. K. *AURORA: A FORTRAN program for modeling well stirred plasma and thermal reactors with gas and surface reactions*; U.S. Department of Energy, Office of Scientific and Technical Information: 1996; DOI: 10.2172/206570.
(33) Shaddix, C. R.; Wang, H.; Schefer, R. W.; Oefelein, J. C.; Pickett, L. M. *Predicting the Effects of Fuel Composition and Flame Structure on Soot Generation in Turbulent Non-Premixed Flames*; Defense Technical Information Center: 2011.

https://doi.org/10.1021/acs.iecr.2c04578
Ind. Eng. Chem. Res. XXXX, XXX, XXX−XXX